

## Weak localization in a GaAs heterostructure close to population of the second subband

J. E. Hansen, R. Taboryski,\* and P. E. Lindelof

*Niels Bohr Institute, The Ørsted Laboratory, University of Copenhagen, Universitetsparken 5, DK-2100 Copenhagen Ø, Denmark*

(Received 29 September 1992; revised manuscript received 5 February 1993)

Weak-localization magnetoresistance has been measured as a function of carrier density using a back-gate technique. The phase relaxation rate and the spin-orbit relaxation rate have been determined. The dominating contribution to the phase relaxation rate comes from electron-electron interaction, as demonstrated for samples covering densities from  $2.5$  to  $7.5 \times 10^{15} \text{ m}^{-2}$ . Interband scattering is found to enhance phase relaxation. A strictly two-dimensional electron gas (2DEG) quenches the spin-orbit relaxation rate in the plane of the 2DEG,  $1/\tau_{\text{so}}^{x,y}$ , whereas the orthogonal part,  $1/\tau_{\text{so}}^z$ , appears added to the phase relaxation rate in the interpretation of the weak-localization magnetoresistance, and can be determined as the saturation value of the phase relaxation at low temperatures. For high carrier densities, intersubband scattering makes the spin-orbit scattering more isotropic and our data support a theory by Elliott.

Two-dimensional electronic gas (2DEG) systems may be realized in two fundamentally different ways. In a strict sense the 2DEG has only one eigenenergy for the electrons in the  $z$  direction. This is a situation for electrons in a thin quantum well with only one subband occupied, as exemplified by Si metal-oxide-semiconductor field-effect transistors and GaAs modulation-doped heterostructures. The other type of 2DEG is found in thin metal films, for which the phase coherence length is much longer than the layer thickness. The phase coherence length for a strictly 2DEG is  $\Lambda_\phi = \sqrt{D\tau_\phi}$ , with  $D = v_F^2\tau_0/2$ , where  $v_F$  is the Fermi velocity and  $\tau_0$  is a total scattering rate for electrons, which we in the following take as the transport relaxation rate.  $\tau_\phi$  is the decay time of the phase of the electrons and related to the inelastic scattering time.

A two-dimensional system is referred to as weakly localized, if the mean free path of the electrons,  $v_F\tau_0$ , is much longer than the de Broglie wavelength  $h/(mv_F)$ . For such systems one observes a decrease in the electrical conductance  $\Delta\sigma = -(e^2/\pi h)\ln(\tau_\phi/\tau_0)$  as temperature and consequently  $1/\tau_\phi$  decreases. Weak localization has been studied in metal films<sup>1</sup> as well as in strict two-dimensional semiconductor systems.<sup>2,3</sup>

Since the contribution of weak localization to the conductivity is not easily distangled from other contributions, such as the electron-electron interaction, most studies of weak localization have relied on measurements of magnetoconductance at low magnetic fields for which weak localization often gives a dominating and characteristic contribution first calculated by Hikami, Larkin, and Nagaoka:<sup>4</sup>

$$-\delta\sigma(B) = (e^2/\pi h) \left\{ \psi\left(\frac{1}{2} + B_0/B\right) - \psi\left(\frac{1}{2} + B_1/B\right) + 0.5\psi\left(\frac{1}{2} + B_2/B\right) - 0.5\psi\left(\frac{1}{2} + B_3/B\right) \right\}, \quad (1)$$

where  $B_1 = B_\phi + B_{\text{so}}^x + B_{\text{so}}^y + B_{\text{so}}^z$ ,  $B_2 = B_\phi$ , and  $B_3 = B_\phi + 2B_{\text{so}}^x + 2B_{\text{so}}^y$ . In terms of the relevant scattering times  $\tau_0$ ,  $\tau_\phi$ , and the anisotropic spin-orbit scattering

times  $\tau_{\text{so}}^x, \tau_{\text{so}}^y, \tau_{\text{so}}^z$ , the characteristic fields can be written  $B_0 = h/(8\pi eD\tau_0)$ ,  $B_{\text{so}}^{x,y,z} = h/(8\pi eD\tau_{\text{so}}^{x,y,z})$ , and  $B_\phi = h/(8\pi eD\tau_\phi)$ .  $B$  is the external magnetic field perpendicular to the two-dimensional layer and  $\psi(x)$  is the digamma function. In Eq. (1) it is assumed that there is no magnetic scattering and that the elastic scattering time  $\tau_0$  is much shorter than the other characteristic times. Equation (1) is applicable to both the above types of two-dimensional electron systems. In metallic films the spin-orbit scattering is normally taken to be isotropic,<sup>1</sup> which leads to  $B_{\text{so}} = 3B_{\text{so}}^x = 3B_{\text{so}}^y = \frac{3}{2}B_{\text{so}}^z$ . The spin-orbit effects measured<sup>5-7</sup> in thin metal films are so far only semiquantitatively understood. In the strict two-dimensional case the spin-orbit interaction gives only a dephasing component perpendicular to the 2DEG, i.e.,  $B_{\text{so}}^x = B_{\text{so}}^y = 0$ . This means that  $B_2 = B_3$  and the shape of the weak localization magnetoresistance cannot be distinguished from the case where there is no spin-orbit effect. However, the existence of  $B_{\text{so}}^z \neq 0$  will lead to a residual value of  $B_1$  at low temperatures, where we expect  $B_\phi$  to vanish. In the strict two-dimensional electron systems the experimental situation has been puzzling. The signature of the spin-orbit interaction has been measured repeatedly in the two-dimensional electron systems at a heterojunction interface,<sup>8-13</sup> and there has been, in spite of the theoretical predictions in Ref. 4, considerable debate about the relevance of spin-orbit scattering to weak localization magnetoresistance. In the following we present measurements which confirm the importance of electron-electron scattering for phase relaxation at low temperatures, and which shed new light on the role of spin-orbit effects on weak localization in a semiconductor 2DEG.

We have used a back gate technique<sup>14</sup> to study weak localization magnetoresistance for several different carrier densities. The samples were modulation-doped GaAs/Al<sub>0.30</sub>Ga<sub>0.70</sub>As heterostructures with undoped Al<sub>0.30</sub>Ga<sub>0.70</sub>As space layers. The two-dimensional electron system was confined by mesa etch in a conventional Hall bar geometry with a width of 0.4 mm. The Au back gate covered all the back surface of the chip. The back

gate voltage could be frozen at a number of values ( $\pm 85$ ,  $\pm 150$ ,  $\pm 200$  V) at room temperature and the sample then cooled to helium temperature in order to have stable and reproducible results. See Table I for the properties of the investigated samples as well as samples from Refs. 11 and 12. The fact that the distance from the back gate to the two-dimensional electrons is comparable to the width of the etched mesa meant that the capacitively induced electrons had a density which varied slightly across the 0.4-mm-wide mesa. We have used the Shubnikov-de Haas oscillations for the determination of the densities. At gate voltages higher than 200 V, the tiny weak localization magnetoresistance could not be reproducibly measured; however, here a beat was observed in the Shubnikov-de Haas oscillations, indicating a second subband being populated. For sample No. 2 an almost constant population,  $n_1 \sim 7 \times 10^{15} \text{ m}^{-2}$  was observed for the lowest subband and for voltages higher than 200 V. The critical electron density, where the second subband began to fill, was therefore taken to be  $7 \times 10^{15} \text{ m}^{-2}$ .

Transport at the transition from populating one to two subbands has been studied experimentally<sup>15-17</sup> and theoretically<sup>18-21</sup> earlier in the literature, but so far with no quantitative comparisons. Our weak localization magnetoresistance experiments were carried out at 4.2 and 1.2 K using a sensitive dc Wheatstone bridge. Figure 1 shows three magnetoresistance curves for sample No. 2 for different back gate voltages. The curves are all experimental traces taken on an X-Y recorder. Such magnetoresistance curves were fitted to Eq. (1) with an isotropic spin-orbit field  $B_{so}$  and a phase relaxation field  $B_\phi$ .  $B_0$  was determined from the zero field resistivity and the carrier density. Since  $B_\phi$  decreases faster with increasing  $n$  than  $B_{so}$ , the double-peak magnetoresistance, which

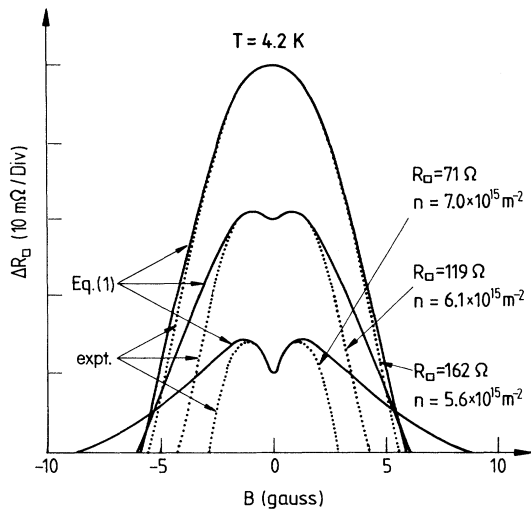


FIG. 1. Weak localization magnetoresistance of sample No. 2 as a function of magnetic field. The present gate voltages are  $-200$ ,  $-85$ , and  $+150$  V.  $T=4.2$  K. The divisions along the y axis amount to only 14, 8, and  $6 \times 10^{-5}$  of the square resistance. Such curves are fitted to the theory of Hikami, Larkin, and Nagaoka (Ref. 4), Eq. (1), and the phase and spin-orbit relaxation times for these three as well as all other investigated samples are given in Table I.

TABLE I. Parameters for the 2DEG in four GaAs/Ga<sub>x</sub>Al<sub>1-x</sub>As samples, Nos. 1-4 (from four different wafers), investigated by us and parameters from samples in Refs. 11 and 12. Data are for  $T=4.2$  K or, if in parenthesis, at  $T=1.2$  K.  $R_S$  is the square resistance in  $\Omega$ ;  $B_0$ ,  $B_\phi$ , and  $B_{so}$ , which are derived from experiments using Eq. (1), are in units of  $\mu\text{T}$ .

$V_G$	$n$	$R_S$	$B_0$	$B_\phi$	$B_{so}$
Sample No. 1, $T=4.2$ K					
-200	2.3	247	428	314	
0	2.8	117	117	90	
200	3.3	65	43	47	
Sample No. 2, $T=4.2$ K (1.2 K)					
-200	5.5	162	451	80	42
-150	5.8	142	359	62	35
-85	6.1	119	264	48	36
0	6.4	95	174	33(14)	26(22)
85	6.6	77	123	29(14)	22(20)
150	7.0	71	110	26	19
200	7.4	69	107	29	21
Sample No. 3, $T=4.2$ K (1.2 K)					
0	7.0	128	402	45(28)	37(33)
Sample No. 4, $T=4.2$ K (1.2 K)					
-200	6.5	120	263	39(18)	42(40)
0	7.2	79	139	24(12)	30(29)
200	7.9	61	84	16(11)	23(22)
Samples from Ref. 11, $T=4.2$ K (1.2 K)					
No. 1	3.7	80	71	27(15)	
No. 2	3.5	113	138	42(20)	
No. 3	3.4	135	194	59(27)	
No. 4	3.2	360	290	240(86)	
Samples from Ref. 12, $T=4.2$ K					
1016	6.4	224			33
1016	6.4	130			30
1017	6.1	96			30
G131	5.6	153			27

characterizes a dominating spin-orbit effect at low magnetic fields, is enhanced as  $n$  increases. Table I gives the determined parameters for the four samples investigated as well as parameters for samples from Refs. 11 and 12. The fact that  $B_{so}$  decreases with increasing  $n$  is opposite to the recent findings of Ref. 12. However we emphasize that  $1/\tau_{so}$  increases with  $n$  in both cases.

In Fig. 2 the experimentally determined values of  $1/\tau_\phi$  for the samples of this investigation at several gate voltages and some earlier results of Ref. 11 are plotted as a function of the two-dimensional carrier density. Note in particular the nonmonotonic variation at the highest carrier density close to the population of the second subband. The phase-breaking length is dominated by electron-electron scattering, which takes different expressions depending on whether  $k_B T > h/2\pi\tau_0$  (clean limit) or  $k_B T < h/2\pi\tau_0$  (dirty limit). The analysis of Ref. 11 gives for a sample with a mobility of  $5.4 \text{ m}^2/\text{Vs}$  (scattering rate  $48 \times 10^{10} \text{ s}^{-1}$ ) the following expression for the phase relaxation rate:<sup>11</sup>

$$\begin{aligned}
 1/\tau_\phi &= 1/\tau_N + 1/\tau_{ee} + \delta \\
 &= k_B T / (2E_F \tau_0) \ln(2\pi E_F \tau_0 / h) + F^2 \pi^2 k_B^2 T^2 / (h E_F) \ln(2\pi E_F \tau_0 / h) + \delta \\
 &= (27T/n^3 + 0.7T^2/n + 2.7) 10^{10} \text{ s}^{-1},
 \end{aligned} \tag{2}$$

where we have assumed that  $h/2\pi\tau_0 > k_B T$ . In the last expression we have used that  $E_F \sim n$ ,  $\tau_0 \sim n^2$  (from experiment) and the coupling constant  $F=0.58$ .<sup>11</sup>  $T$  is in units of K and  $n$  in units of  $10^{15} \text{ m}^{-2}$ . The last term is a phenomenological scattering rate which in Ref. 11 was introduced to match the fact that  $\tau_\phi$  saturates at a finite value as the temperature goes towards zero. We believe that this constant value at low temperatures reflects the addition of  $1/\tau_{so}^z$  to  $1/\tau_\phi$  for the strictly (or in the case of a thin metallic film, anisotropic) 2DEG in Eq. (1) as already mentioned above. Ideally, at the transition to the second subband,  $n_c = 7 \times 10^{15} \text{ m}^{-2}$  (sample No. 2), we expect a doubling of the density of states due to the appearance of the second subband. However a smeared transition is expected due to scattering lifetime effects, sample inhomogeneities and temperature. The electron-electron scattering rates [clean and dirty limit expressions in Eq. (2)] at one particular energy is expected to be proportional to the density of states and therefore abruptly doubles at  $n_c$ . In order to obtain a realistic graph of the total phase relaxation rate versus  $n$ , we assume a smearing in carrier density of  $0.5 \times 10^{15} \text{ m}^{-2}$  (roughly 1 meV on the energy scale) according to the following expression:

$$\begin{aligned}
 \langle 1/\tau_\phi(n) \rangle &= \frac{2}{\sqrt{\pi}} \int_{-\infty}^7 \tau_\phi^{-1}(n') e^{-4(n-n')^2} dn' \\
 &+ \frac{2}{\sqrt{\pi}} \int_7^{\infty} \tau_\phi^{-1}(n') e^{-4(n-n')^2} dn'.
 \end{aligned} \tag{3}$$

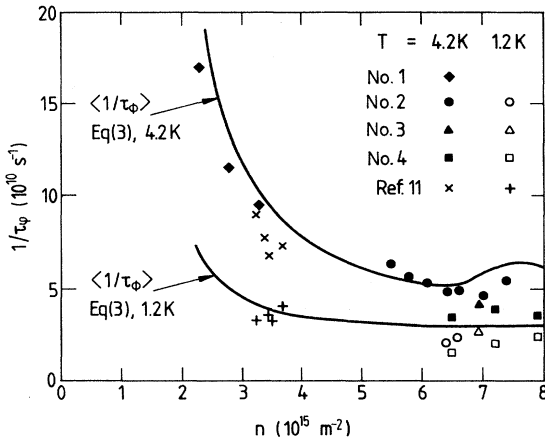


FIG. 2. The phase relaxation rate for samples Nos. 1–4 and from Ref. 11 plotted as a function of two-dimensional carrier density. Data for the two temperatures  $T=4.2$  and  $1.2$  K are displayed. The phase relaxation rates at  $1.2$  K are close to the low-temperature saturation value, which in Eq. (3) is set to  $2.7 \times 10^{10} \text{ s}^{-1}$ . The curves are the theoretical expression for the electron-electron scattering rate calculated in Ref. 11 and given by Eqs. (2) and (3). The electron-electron scattering rate doubles above the carrier density where the second subband starts to fill and  $1/\tau_\phi$  is smeared with a Gaussian function with an energy half-width of 1 meV as given by Eq. (3).

In Fig. 2  $\langle 1/\tau_\phi \rangle$  is shown as the full lines for the temperatures  $T=4.2$  and  $1.2$  K. The agreement between model and experiment is quite satisfactory considering that we have modified the dirty limit formula for the different mobilities of the 2DEG's. We may question the use of Eq. (1) for analyzing the situation where the second subband begins to be populated,<sup>21</sup> because spin-orbit effects are expected to be anisotropic ( $\tau_{so}^z > 2\tau_{so}^x$ ). In the carrier density region where the second subband is populated we believe that Eq. (1) with an isotropic spin-orbit field becomes more valid. The experimentally determined  $1/\tau_{so}$  is therefore expected to increase as the second subband begins to populate and then at higher carrier densities to become constant. Simultaneously we expect the temperature-independent part of  $1/\tau_\phi$  ( $1/\tau_{so}^z$ ) to be absorbed in the isotropic  $1/\tau_{so}$ . This is in fact what we observe.

There are (at least) three possible sources of spin-orbit interaction, which can be the origin of the spin-orbit dephasing: (1) scattering against heavy impurities,<sup>22</sup> (2) scattering associated with the electric field of impurities,<sup>23</sup> and (3) scattering in materials with spin-split energy levels.<sup>24,12</sup> According to Ref. 12 the last contribution may explain the origin of the spin-orbit scattering. However, we do not find the quadratic dependence of  $B_{so}$  versus  $n$  which is reported in Ref. 12. We find indeed much better agreement with the expression given in Ref.

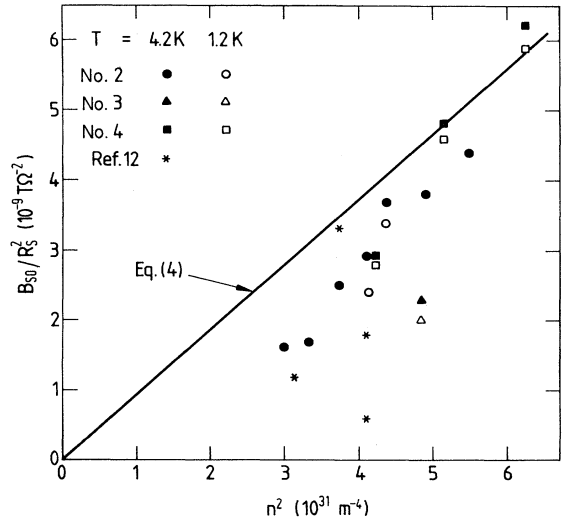


FIG. 3.  $B_{so}/R_S^2$  plotted vs  $n^2$  for 2DEG's exhibiting spin-orbit effect in the weak localization magnetoresistance. Samples Nos. 2–4 and data from Ref. 12 are plotted. Only for carrier densities above  $5.5 \times 10^{15} \text{ m}^{-2}$ , i.e., close to population of the second subband (at  $7 \times 10^{15} \text{ m}^{-2}$  for sample No. 2) is spin-orbit effects observed in the magnetoresistance. The straight line is calculated from Eq. (5) with  $R=1.2$  nm. Measurements at  $4.2$  and  $1.2$  K are shown.

23, which can be expressed in the following way:

$$B_{\text{so}}/R_S^2 = n^2(g-2)^2 R^2 D(E_F) h e^3 / m. \quad (4)$$

Here  $D(E_F)$  is the density of states,  $R$  is the diameter of the impurity scatterer,  $m$  is the effective electron mass ( $0.07m_0$ ), and  $g$  is the electronic  $g$  factor,  $g \approx 0.4$  for the conduction band in GaAs. In Fig. 3 we have plotted our experimental values of  $B_{\text{so}}/R_S^2$  as well as four values extracted from Ref. 12 (see Table I) as a function of  $n^2$ . The line predicted by Eq. (4) is drawn through the points at the highest carrier density, where  $1/\tau_{\text{so}}$  is expected to be closest to the isotropic value. The slope of this line gives  $R = 1.2$  nm. This is a reasonable value for the size of an impurity scatterer.

In conclusion we emphasize that the phase relaxation rate is well described by electron-electron interaction at

low temperatures. In this paper we have emphasized the carrier density dependence, whereas earlier experiments have focused on the temperature and mobility dependence.<sup>11</sup> The problem around the spin-orbit effects in the weak localization of semiconductor 2DEG is not settled. We have interpreted our results in the light of the anisotropic spin-orbit effect, which has not previously been experimentally investigated. Our results point to the importance of interband scattering which, if strong enough, makes spin-orbit scattering isotropic. Our results at high carrier densities support the theory by Elliott.<sup>23</sup> More theoretical work on spin-orbit scattering is, however, needed in order to clarify the results of weak localization experiments.

We acknowledge the technical assistance of J. Brinchmann and M. Bøgelund Jensen.

\*Permanent address: Ferroperm A/S, Stubbeled 7, DK-2950 Vedbaek, Denmark.

<sup>1</sup>G. Bergmann, Phys. Rep. **107**, 1 (1984).

<sup>2</sup>S. Kawaji, Surf. Sci. **170**, 682 (1986).

<sup>3</sup>P. E. Lindelof, J. Nørregaard, and J. Hanberg, Phys. Scr. **T14**, 17 (1987).

<sup>4</sup>S. Hikami, A. I. Larkin, and Y. Nagaoka, Prog. Theor. Phys. **63**, 707 (1980); for a recent theoretical review see J. Rammer, Rev. Mod. Phys. **63**, 781 (1991).

<sup>5</sup>G. Bergmann, Phys. Rev. Lett. **48**, 1046 (1982).

<sup>6</sup>M. Gijs, C. van Haesendonck, Y. Bruynseraede, and G. Deucher, in *Proceedings of the International Conference on Localization, Interaction, and Transport Phenomena in Impure Metals*, edited by X. Schweitzer and Y. Kramer (PTB, Braunschweig, 1984), p. 139.

<sup>7</sup>P. E. Lindelof and S. Wang, Phys. Rev. B **33**, 1478 (1986); S. Wang and P. E. Lindelof, J. Low Temp. Phys. **71**, 403 (1988).

<sup>8</sup>D. A. Poole, M. Pepper, and A. Hughes, J. Phys. C **15**, L1137 (1982).

<sup>9</sup>S. Kawaji, K. Kuboki, H. Shigeno, T. Nambu, J. Wakabayashi, J. Yoshino, and H. Sakaki, in *17th International Conference on the Physics of Semiconductors*, edited by J. D. Chadi and W. A. Harrison (Springer, New York, 1985), p. 413.

<sup>10</sup>Y. Kawaguchi, I. Takayanagi, and S. Kawaji, J. Phys. Soc. Jpn. **56**, 1293 (1987).

<sup>11</sup>R. Taboryski and P. E. Lindelof, Semicond. Sci. Technol. **5**, 933 (1990).

<sup>12</sup>P. D. Dresselhaus, C. M. A. Papavassiliou, R. G. Wheeler, and R. N. Sacks, Phys. Rev. Lett. **68**, 106 (1992).

<sup>13</sup>Wiley Kirk (private communication).

<sup>14</sup>H. L. Störmer, A. C. Gossard, and W. Wiegmann, Appl. Phys. Lett. **39**, 493 (1981).

<sup>15</sup>H. L. Störmer, A. C. Gossard, and W. Wiegmann, Solid State Commun. **41**, 707 (1982).

<sup>16</sup>J. C. Portal, R. J. Nicholas, M. A. Brummell, A. Y. Cho, K. Y. Chang, and T. D. Pearsall, Solid State Commun. **43**, 907 (1982).

<sup>17</sup>T. Englert, J. C. Maan, D. C. Tsui, and A. C. Gossard, Solid State Commun. **45**, 989 (1983).

<sup>18</sup>S. Mori and T. Ando, Phys. Rev. B **19**, 6433 (1979).

<sup>19</sup>N. T. Thang, G. Fishman, and B. Vinter, Surf. Sci. **142**, 266 (1984).

<sup>20</sup>M. J. Kearney and P. N. Butcher, J. Phys. C **21**, 2539 (1988).

<sup>21</sup>S. Iwabuchi and Y. Nagaoka, J. Phys. Soc. Jpn. **58**, 1325 (1989).

<sup>22</sup>A. A. Abrikosov and L. P. Gorkov, Zh. Eksp. Teor. Fiz. **42**, 1088 (1962) [Sov. Phys. JETP **15**, 752 (1962)].

<sup>23</sup>R. J. Elliott, Phys. Rev. **96**, 266 (1954).

<sup>24</sup>M. I. Dyakanov and V. I. Perel, Zh. Eksp. Teor. Fiz. **60**, 1954 (1971) [Sov. Phys. JETP **33**, 1053 (1971)].